Reactance of hollow, solid, and hemispherical-cap cylindrical posts in rectangular waveguide

J Roelvink* Allan Williamson†

*University of Auckland,

†University of Auckland, ag.williamson@auckland.ac.nz

Reactance of Hollow, Solid, and Hemispherical-Cap Cylindrical Posts in Rectangular Waveguide

J. Roelvink, *Student Member, IEEE,* and Allan G. Williamson, *Senior Member, IEEE*

***Abstract*—An accurate experimental technique is employed to determine the reactance of three commonly used symmetrical waveguide discontinuities: cylindrical posts with hollow, solid, and hemispherical-cap ends, and a useful data set is presented. Length adjustment factors are derived for the case of symmetrical excitation that relate the reactance of each post form. When used in conjunction with an existing analysis, it is shown that very accurate results can be predicted for the reactance of solid and hemispherical-cap posts.**

***Index Terms*—Filters, tuning networks, waveguides.**

I. Introduction

ONE OF the most commonly used reactive elements in waveguide matching and filter networks is a cylindrical metallic post that extends into the waveguide, as shown in Fig. 1(a). The post axis is orientated parallel to the dominant TE_{10}-mode electric field. The current distribution induced on the post by the incident TE_{10} mode will depend on the physical dimensions of the waveguide and the size and form of the post itself; hollow, solid, or hemispherical cap. By changing ℓ, the induced current and, hence, the reactive effect of the post, can be adjusted (in practice, this is usually facilitated by using a threaded post that enters through a threaded hole in the waveguide). Notwithstanding its widespread use, there is little published data for the reactance of cylindrical posts other than in [1] where experimental data is given for solid and hemispherical-cap posts. Over the years, these measurements have received many citations.

In the full-height case, when $\ell = h$, the axial current induced by the incident TE_{10} mode is constant along the post surface, significantly reducing the difficulty of the theoretical analysis. Schwinger and Saxon solved this problem using a variational procedure [2] by approximating the circumferential variation of the axial current around the post by two terms of a Fourier series, the results of which appear in [1]. Leviatan *et al.* [3] also considered the full-height case by representing the post as a number of filaments and solving the boundary conditions using a point-matching technique. This analysis allows the circumferential variation of the induced axial current around the post to be approximated to a high order, making it very accurate for posts up to large radii. Their results were shown to be in good agreement with Schwinger's theoretical analysis within his stated bounds of accuracy.

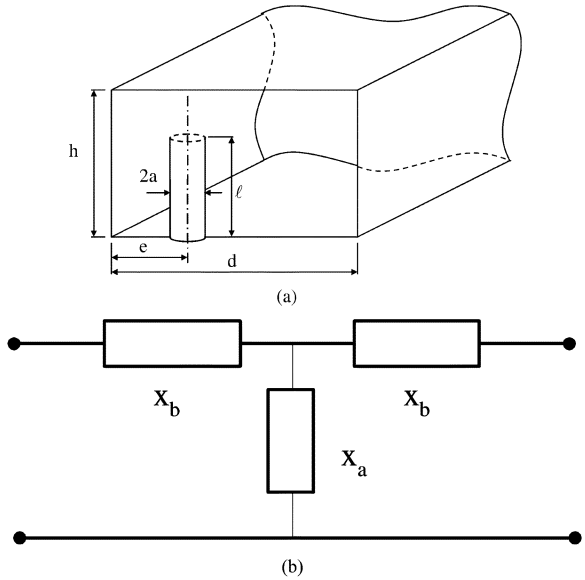

Fig. 1. (a) Variable-length post sectional view. (b) T-equivalent circuit.

In the variable-length case, when $\ell \neq h$, the axial current induced by the incident TE_{10} mode is no longer constant along the post, significantly increasing the complexity of any theoretical analysis. One of the earliest studies was by Lewin [4] who represented the post current by a filament with an assumed sinusoidal distribution. A more accurate theoretical analysis was developed by Williamson [5] for the analytically tractable case of a hollow post. Unlike Lewin, no assumption was made about the form of the induced current, although the effect of the circumferential variation around the post surface was averaged, making the analysis applicable to relatively thin posts only. More recently, an analysis has been reported [6] in which the post is approximated as a prism consisting of a number of strips each carrying an axial current.

In practice, the post would most likely be solid or, for high power applications, have a hemispherical cap. It would be expected that the reactance of a hollow, solid, or hemispherical-cap post of a certain length would only be slightly different, and the variation of the reactance of each form as a function of the physical dimensions and position would be very similar. Indeed, it might be expected that the reactance of one form could be closely represented by that of another of a slightly different length. If this length adjustment was known, then data available for one form could be used to predict the reactance values for others. Moreover, the theoretical treatment in [5] could then be

Manuscript received February 2, 2005; revised May 14, 2005. The work of J. Roelvink was supported by Technology New Zealand under a Technology in Industry Award.

The authors are with the Department of Electrical and Computer Engineering, The University of Auckland, Auckland, New Zealand (e-mail: jroe003@ec.auckland.ac.nz).

Digital Object Identifier 10.1109/TMTT.2005.855356

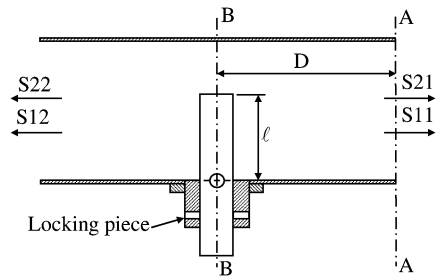

Fig. 2. Experimental test setup.

used to predict reactance results for solid and hemispherical-cap posts.

In this paper, a simple and accurate experimental procedure for finding the reactance of symmetrical waveguide discontinuities is used to obtain a data set for the reactance of hollow, solid, and hemispherical-cap posts in a rectangular waveguide. The experimental data set is then used to produce length adjustment factors, relating the reactance of solid and hemispherical-cap posts to hollow posts. Using these length adjustments with the theory in [5], it is shown that the reactance of solid, hollow, and hemispherical-cap posts can be predicted very accurately.

II. Experimental Procedure

The effect of a symmetrical discontinuity, located at some point in a waveguide, can be modeled by the T-equivalent circuit in Fig. 1(b) as with any symmetrical lossless two-port network. By considering an incident wave at one port and assuming that the other is terminated in a perfect match, it is possible to show that [3]

$$jx_a = \frac{2\tau}{(1-\rho)^2 - \tau^2} \tag{1}$$

$$jx_b = -\frac{\rho - \tau + 1}{\rho - \tau - 1} \tag{2}$$

where x_a and x_b are normalized reactances, and ρ and τ are the reflection and transmission coefficients, respectively, relative to the central plane of the discontinuity.

An experimental study was conducted to obtain the S-parameters of five different diameter posts ($2a = 15, 12, 9, 6,$ and 3 mm) within a C-band waveguide ($d = 47.55$ mm, $h = 22.15$ mm) over the usual operating frequency range of the waveguide (3.95–5.85 GHz) using an Agilent PNA series network analyzer. The posts and waveguide test setup were constructed from brass. Due to practical limitations, hemispherical-cap posts were considered for only the two largest post diameters and hollow posts for only the three largest post diameters. The experimental setup is shown in Fig. 2 and was calibrated to the plane A–A (at the connection between the network analyzer port hardware and the waveguide test section) by a thru-reflect line (TRL) calibration. The reference plane was subsequently shifted a length D to the plane B–B at the central plane of the discontinuity. Since the cylindrical post is symmetrical about B–B, in theory, $S_{11} = S_{22}$ and $S_{12} = S_{21}$. In practice, there was a slight difference due to small imperfections in the experimental setup and, thus, the average of S_{11} and S_{22}, and S_{21} and S_{12} was used as the reflection and transmission coefficients, respectively.

TABLE I
$2a = 3$ mm ($2a/d = 0.063$), Solid Post

ℓ/h	3.95GHz		4.90GHz		5.85GHz	
	x_a	x_b	x_a	x_b	x_a	x_b
0.090	-48.14	-0.001	-52.14	-0.002	-44.23	-0.002
0.181	-12.28	-0.003	-12.14	-0.004	-10.45	-0.005
0.271	-4.826	-0.004	-4.546	-0.006	-3.631	-0.008
0.361	-2.320	-0.006	-2.029	-0.009	-1.421	-0.011
0.451	-1.247	-0.007	-0.994	-0.011	-0.503	-0.014
0.542	-0.698	-0.009	-0.472	-0.013	-0.072	-0.017
0.632	-0.397	-0.010	-0.191	-0.015	0.141	-0.020
0.722	-0.221	-0.011	-0.033	-0.018	0.248	-0.023
0.767	-0.156	-0.013	0.025	-0.019	0.283	-0.025
0.813	-0.101	-0.013	0.064	-0.020	0.308	-0.026
0.858	-0.057	-0.014	0.108	-0.022	0.330	-0.028
0.903	-0.014	-0.015	0.133	-0.023	0.345	-0.029
0.948	0.034	-0.016	0.172	-0.024	0.366	-0.031
1	0.205	-0.016	0.340	-0.027	0.484	-0.034

TABLE II
$2a = 6$ mm($2a/d = 0.126$), Solid Post

ℓ/h	3.95GHz		4.90GHz		5.85GHz	
	x_a	x_b	x_a	x_b	x_a	x_b
0.090	-23.09	-0.004	-23.31	-0.006	-21.96	-0.008
0.181	-6.746	-0.009	-6.704	-0.013	-5.861	-0.016
0.271	-2.806	-0.013	-2.664	-0.020	-2.203	-0.024
0.361	-1.441	-0.018	-1.288	-0.027	-0.923	-0.033
0.451	-0.823	-0.023	-0.666	-0.034	-0.406	-0.042
0.542	-0.494	-0.027	-0.353	-0.041	-0.138	-0.052
0.632	-0.304	-0.032	-0.181	-0.049	-0.003	-0.062
0.722	-0.187	-0.037	-0.081	-0.057	0.080	-0.073
0.767	-0.140	-0.040	-0.043	-0.062	0.107	-0.079
0.813	-0.101	-0.043	-0.009	-0.066	0.132	-0.084
0.858	-0.072	-0.045	0.018	-0.069	0.150	-0.090
0.903	-0.036	-0.047	0.046	-0.074	0.165	-0.095
0.948	0.006	-0.051	0.076	-0.078	0.186	-0.102
1	0.103	-0.054	0.178	-0.083	0.266	-0.109

TABLE III
$2a = 9$ mm ($2a/d = 0.189$), Solid Post

ℓ/h	3.95GHz		4.90GHz		5.85GHz	
	x_a	x_b	x_a	x_b	x_a	x_b
0.090	-13.22	-0.008	-13.91	-0.012	-13.05	-0.013
0.181	-4.116	-0.016	-4.243	-0.025	-3.777	-0.028
0.271	-1.891	-0.026	-1.890	-0.038	-1.607	-0.044
0.361	-1.025	-0.035	-0.998	-0.052	-0.770	-0.059
0.451	-0.623	-0.045	-0.562	-0.066	-0.404	-0.077
0.542	-0.395	-0.055	-0.336	-0.082	-0.189	-0.095
0.632	-0.261	-0.065	-0.207	-0.098	-0.086	-0.116
0.722	-0.172	-0.076	-0.124	-0.116	-0.024	-0.140
0.767	-0.137	-0.082	-0.091	-0.125	0.001	-0.153
0.813	-0.107	-0.088	-0.063	-0.134	0.022	-0.167
0.858	-0.078	-0.093	-0.037	-0.143	0.041	-0.181
0.903	-0.048	-0.099	-0.009	-0.154	0.059	-0.196
0.948	-0.015	-0.105	0.022	-0.164	0.082	-0.212
1	0.050	-0.112	0.092	-0.175	0.147	-0.230

III. Results

Tables I–X present data for the normalized reactances x_a and x_b versus ℓ/h of each post diameter and form at several frequencies. It can be seen that x_a is capacitive at most insertion depths, but becomes inductive for large ℓ/h. Correspondingly,

TABLE IV
$2a = 9$ mm $(2a/d = 0.189)$), HOLLOW POST

ℓ/h	3.95GHz		4.90GHz		5.85GHz	
	x_a	x_b	x_a	x_b	x_a	x_b
0.181	-5.316	-0.011	-5.590	-0.017	-5.093	-0.017
0.271	-2.273	-0.020	-2.351	-0.029	-2.016	-0.032
0.361	-1.186	-0.029	-1.144	-0.043	-0.934	-0.047
0.451	-0.705	-0.038	-0.644	-0.057	-0.477	-0.062
0.542	-0.444	-0.049	-0.390	-0.071	-0.246	-0.079
0.632	-0.292	-0.059	-0.243	-0.088	-0.122	-0.099
0.722	-0.193	-0.070	-0.148	-0.104	-0.049	-0.122
0.767	-0.158	-0.075	-0.115	-0.113	-0.024	-0.134
0.813	-0.125	-0.080	-0.085	-0.122	-0.001	-0.147
0.858	-0.096	-0.086	-0.057	-0.131	0.021	-0.161
0.903	-0.069	-0.092	-0.031	-0.141	0.041	-0.176
0.948	-0.041	-0.098	-0.003	-0.151	0.061	-0.191

TABLE V
$2a = 12$ mm$(2a/d = 0.252)$, SOLID POST

ℓ/h	3.95GHz		4.90GHz		5.85GHz	
	x_a	x_b	x_a	x_b	x_a	x_b
0.090	-8.779	-0.012	-9.554	-0.018	-9.481	-0.020
0.181	-3.032	-0.025	-3.231	-0.036	-3.078	-0.038
0.271	-1.478	-0.040	-1.551	-0.055	-1.416	-0.057
0.361	-0.844	-0.055	-0.871	-0.076	-0.765	-0.076
0.451	-0.536	-0.071	-0.546	-0.098	-0.463	-0.098
0.542	-0.356	-0.087	-0.358	-0.123	-0.298	-0.123
0.632	-0.246	-0.105	-0.246	-0.150	-0.201	-0.156
0.722	-0.169	-0.122	-0.166	-0.181	-0.132	-0.201
0.767	-0.138	-0.131	-0.135	-0.197	-0.102	-0.227
0.813	-0.110	-0.142	-0.105	-0.215	-0.073	-0.257
0.858	-0.084	-0.151	-0.077	-0.233	-0.045	-0.287
0.903	-0.057	-0.161	-0.047	-0.252	-0.015	-0.320
0.948	-0.026	-0.173	-0.011	-0.273	0.020	-0.354
1	0.015	-0.186	0.040	-0.293	0.073	-0.388

TABLE VI
$2a = 12$ mm $(2a/d = 0.252)$, HOLLOW POST

ℓ/h	3.95GHz		4.90GHz		5.85GHz	
	x_a	x_b	x_a	x_b	x_a	x_b
0.181	-4.208	-0.014	-4.556	-0.018	-4.387	-0.016
0.271	-1.835	-0.028	-1.935	-0.036	-1.795	-0.032
0.361	-0.999	-0.042	-1.034	-0.055	-0.919	-0.046
0.451	-0.607	-0.057	-0.620	-0.075	-0.534	-0.063
0.542	-0.405	-0.073	-0.412	-0.097	-0.350	-0.079
0.632	-0.281	-0.089	-0.284	-0.121	-0.244	-0.103
0.722	-0.196	-0.107	-0.200	-0.149	-0.174	-0.136
0.767	-0.163	-0.116	-0.165	-0.165	-0.144	-0.159
0.813	-0.134	-0.125	-0.135	-0.181	-0.117	-0.185
0.858	-0.107	-0.134	-0.107	-0.198	-0.089	-0.215
0.903	-0.083	-0.145	-0.080	-0.216	-0.062	-0.246
0.948	-0.056	-0.155	-0.050	-0.237	-0.030	-0.283

the posts resonate at a certain length, the resonant length increasing for increasing post diameters. The reactance x_b, for electrically thin posts, varies almost linearly with insertion and is small. However, as the post diameter increases, the variation of x_b with insertion no longer behaves linearly and the reactance becomes significant. Consequently, x_b is often referred to as the "post-thickness reactance," as in [7].

The hollow post theory in [5] considers the average electric field incident over the post surface, the boundary condition on the post being applied in that sense. This was shown [5] to give

TABLE VII
$2a = 12$ mm $(2a/d = 0.252)$, HEMISPHERICAL-CAP POST

ℓ/h	3.95GHz		4.90GHz		5.85GHz	
	x_a	x_b	x_a	x_b	x_a	x_b
0.271	-2.834	-0.027	-2.973	-0.039	-2.756	-0.044
0.361	-1.446	-0.042	-1.521	-0.059	-1.372	-0.066
0.451	-0.859	-0.056	-0.894	-0.080	-0.781	-0.087
0.542	-0.541	-0.072	-0.559	-0.103	-0.473	-0.111
0.632	-0.364	-0.088	-0.371	-0.128	-0.306	-0.139
0.722	-0.251	-0.105	-0.255	-0.155	-0.205	-0.173
0.767	-0.206	-0.114	-0.209	-0.170	-0.164	-0.194
0.813	-0.170	-0.123	-0.166	-0.185	-0.129	-0.218
0.858	-0.138	-0.132	-0.132	-0.201	-0.098	-0.243
0.903	-0.107	-0.142	-0.097	-0.219	-0.066	-0.271
0.948	-0.074	-0.153	-0.062	-0.237	-0.033	-0.302

TABLE VIII
$2a = 15$ mm $(2a/d = 0.315)$, SOLID POST

ℓ/h	3.95GHz		4.90GHz		5.85GHz	
	x_a	x_b	x_a	x_b	x_a	x_b
0.090	-7.408	-0.016	-8.213	-0.021	-8.574	-0.022
0.181	-2.513	-0.034	-2.799	-0.043	-2.866	-0.041
0.271	-1.262	-0.053	-1.406	-0.068	-1.409	-0.056
0.361	-0.756	-0.073	-0.846	-0.091	-0.850	-0.068
0.451	-0.492	-0.095	-0.558	-0.119	-0.571	-0.080
0.542	-0.341	-0.118	-0.397	-0.150	-0.429	-0.095
0.632	-0.243	-0.142	-0.291	-0.188	-0.338	-0.128
0.722	-0.173	-0.169	-0.211	-0.235	-0.261	-0.193
0.767	-0.144	-0.183	-0.177	-0.262	-0.221	-0.241
0.813	-0.117	-0.197	-0.144	-0.290	-0.180	-0.299
0.858	-0.091	-0.212	-0.111	-0.321	-0.133	-0.367
0.903	-0.064	-0.229	-0.076	-0.355	-0.085	-0.438
0.948	-0.035	-0.245	-0.038	-0.389	-0.033	-0.510
1	0.009	-0.265	0.014	-0.428	0.034	-0.579

TABLE IX
$2a = 15$ mm $(2a/d = 0.315)$, HOLLOW POST

ℓ/h	3.95GHz		4.90GHz		5.85GHz	
	x_a	x_b	x_a	x_b	x_a	x_b
0.271	-1.689	-0.030	-1.890	-0.030	-1.932	-0.009
0.361	-0.924	-0.049	-1.039	-0.050	-1.046	-0.010
0.451	-0.595	-0.068	-0.680	-0.070	-0.698	-0.002
0.542	-0.405	-0.089	-0.476	-0.094	-0.525	0.012
0.632	-0.289	-0.112	-0.353	-0.122	-0.436	0.028
0.722	-0.211	-0.136	-0.271	-0.158	-0.386	0.029
0.767	-0.180	-0.149	-0.236	-0.179	-0.361	0.018
0.813	-0.152	-0.162	-0.204	-0.203	-0.335	-0.009
0.858	-0.125	-0.177	-0.172	-0.231	-0.301	-0.053
0.903	-0.099	-0.194	-0.138	-0.264	-0.255	-0.120
0.948	-0.075	-0.208	-0.107	-0.295	-0.208	-0.196

accurate results for the average axial surface current, but neglects the circumferential variation around the post (and, thus, $\tau = 1 + \rho$ and $x_b = 0$). However, for the case of symmetrical excitation, the circumferential variation of the current would be somewhat lessened and it might be expected that the theory in [5] would accurately model that situation. For symmetrical excitation, the equivalent circuit of Fig. 1(b) would reduce to a single reactance $x_T = x_a + x_b/2$.

IV. LENGTH ADJUSTMENT FACTORS

Fig. 3 presents a graph of x_T for the three post forms considered in this study. It can be seen that the physical differences of

TABLE X
$2a = 15$ mm ($2a/d = 0.315$), HEMISPHERICAL-CAP POST

ℓ/h	3.95GHz		4.90GHz		5.85GHz	
	x_a	x_b	x_a	x_b	x_a	x_b
0.361	-1.29	-0.055	-1.420	-0.076	-1.384	-0.077
0.451	-0.78	-0.076	-0.875	-0.104	-0.858	-0.099
0.542	-0.51	-0.098	-0.580	-0.133	-0.582	-0.122
0.632	-0.36	-0.120	-0.413	-0.166	-0.428	-0.150
0.722	-0.25	-0.145	-0.297	-0.205	-0.320	-0.193
0.767	-0.21	-0.157	-0.252	-0.226	-0.277	-0.222
0.813	-0.18	-0.171	-0.210	-0.251	-0.235	-0.259
0.858	-0.14	-0.185	-0.173	-0.276	-0.194	-0.303
0.903	-0.11	-0.200	-0.134	-0.305	-0.149	-0.356
0.948	-0.08	-0.216	-0.093	-0.336	-0.099	-0.416

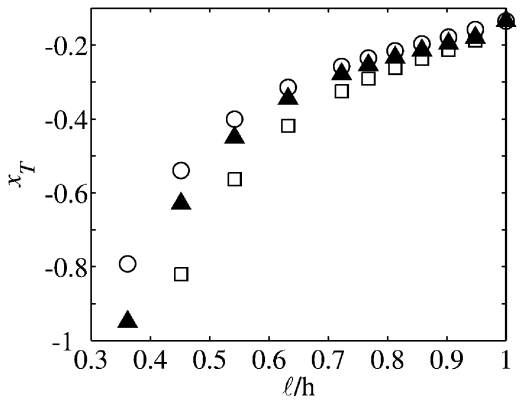

Fig. 3. Experimental results for the variable-length cylindrical post reactance x_T as a function of ℓ/h. $h = 22.15$ mm, $d = 47.55$ mm, $e/d = 0.5, 2a = 15$ mm, and $f = 3.95$ GHz ∘ ∘ ∘: solid post. □□□: hemispherical-cap post. ▲▲▲: hollow post.

the post ends translate to a slight offset in the reactance curves, as postulated. If the hollow post was taken as the reference post, it is evident that the solid post has a reactance that corresponds to an "effective hollow length," which is longer than its actual length. In the case of a hemispherical-cap post, the "effective hollow length" is less than the physical length measured to the apex. These differences (between the actual length and effective hollow length, i.e., the length of a hollow post yielding the same x_T reactance value) were calculated from the experimental data for several frequencies and the five different post diameters. Essentially the same result was found at each frequency and, accordingly, it was concluded that the adjustment factor was principally only a function of the post radius. It was found that to a very good approximation (ℓ_s and ℓ_c), the effective hollow length of solid and hemispherical-cap posts of length ℓ are given by

$$\ell_s \approx \ell + 0.12a \tag{3}$$

$$\ell_c \approx \ell - 0.24a. \tag{4}$$

This result accurately models the situation shown in Fig. 3, except when the post end is very close to the upper surface of the waveguide, i.e., when ℓ approaches h and for small insertions of the hemispherical-cap post, when $\ell < a$ (in many practical applications, these regions would be avoided and, thus, (3) and (4) are largely sufficient at characterizing the difference in reactance).

The above results, i.e., (3) and (4), were deduced from the scattered fields (far fields) of cylindrical posts in a rectangular waveguide. It is interesting to note that they are in good agreement with previously published results for a different situation. Lee and Mittra [8] and Ting [9] considered the case of a cylindrical antenna in free space driven by a coaxial line, and by comparing the input admittance (which depends on the near fields) of hollow and solid and hollow and hemispherical-cap antennas, respectively, deduced length adjustment factors of $+0.13a$ and $-0.25a$.

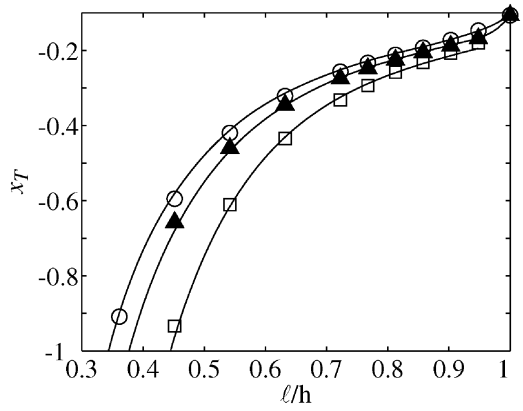

Fig. 4. Theoretical and experimental results for the variable-length cylindrical post reactance x_T as a function of ℓ/h. $h = 22.15$ mm, $d = 47.55$ mm, $e/d = 0.5, 2a = 12$ mm, and $f = 4.90$ GHz. ——: theoretical results using length adjustment factors and [5]. ∘ ∘ ∘: experimental results for solid post. □□□: experimental results for hemispherical-cap post. ▲▲▲: experimental results for hollow post.

V. COMPARISON OF THEORETICAL AND EXPERIMENTAL VALUES FOR x_T

If the experimentally derived adjustment factors, i.e., (3) and (4), are now applied to the hollow post theory in [5], it should be possible to predict the reactance of solid and hemispherical-cap posts. Theoretical results for the reactance x_T obtained in this manner are shown in Fig. 4 along with the experimental measurements of the three post forms. The accuracy of the length adjustment factors is evident even when the post insertion is quite large. Furthermore, it is interesting that the results for x_T for hollow posts are quite accurate even for the electrically thick posts, up to 32% the waveguide width, that were considered in this study.

VI. CONCLUSION

An accurate means of measuring the reactance of variable-length cylindrical posts in a rectangular waveguide has been used that could easily be applied to other waveguide discontinuities and cross sections. This has permitted a useful data set to be obtained. Furthermore, experimentally derived length adjustment factors have been presented that relate the reactance of solid and hemispherical-cap posts to that of a hollow cylindrical post in a rectangular waveguide. These factors are applicable to the case of symmetrical excitation and can be used for relatively thick diameter posts, the largest investigated being over 30% of the waveguide width. When combined with a readily available theory for the reactance of hollow cylindrical posts, theoretical results have been obtained that are in excellent agreement with

the experimental measurements. The knowledge of these factors is of benefit in the practical design of waveguide filters and microwave tuning networks, providing a method for accurately predicting commonly used, but little analyzed reactive elements. Developing a means of analyzing the case of general excitation is a focus of ongoing research by the authors.

ACKNOWLEDGMENT

The authors wish to thank Keam Holdem Associates, Auckland, New Zealand, for being the industrial partner of the Technology New Zealand TIF Award, and Dr. R. Keam, Keam Holdem Associates, for several helpful discussions.

REFERENCES

[1] N. Marcuvitz, Ed., *Waveguide Handbook*. ser. MIT Rad. Lab. New York: McGraw-Hill, 1951, vol. 10, pp. 271–273.

[2] J. Schwinger and D. Saxon, *Discontinuities in Waveguides*. New York: Gordon and Breach, 1968.

[3] Y. Leviatan, P. G. Li, A. T. Adams, and J. Perini, "Single-post inductive obstacle in rectangular waveguide," *IEEE Trans. Microw. Theory Tech.*, vol. MTT-31, no. 10, pp. 806–812, Oct. 1983.

[4] L. Lewin, *Advanced Theory of Waveguides*. London, U.K.: Iliffe, 1951.

[5] A. G. Williamson, "Variable-length cylindrical post in a rectangular waveguide," *Proc. Inst. Elect. Eng.*, pt. H, vol. 133, pp. 1–9, 1986.

[6] Y. Huang, N. Yang, S. Lin, and R. F. Harrington, "Analysis of a post with arbitrary cross section and height in a rectangular waveguide," *Proc. Inst. Elect. Eng.*, pt. H, vol. 138, pp. 475–480, 1991.

[7] A. G. Williamson, "Analysis and modeling of a coaxial-line/rectangular-waveguide junction," *Proc. Inst. Elect. Eng.*, pt. H, vol. 129, pp. 262–270, 1982.

[8] S. W. Lee and R. Mittra, "Admittance of a solid cylindrical antenna," *Can. J. Phys.*, vol. 47, pp. 1959–1970, 1969.

[9] C. Ting, "Theoretical study of a cylindrical antenna with a hemispherical cap," *IEEE Trans. Antennas Propag.*, vol. AP-17, no. 6, pp. 715–721, Nov. 1969.

J. Roelvink (S'02) was born in Auckland, New Zealand, in 1981. He received the B.E. degree in electrical and electronic engineering (with first-class honors) from the University of Auckland, Auckland, New Zealand, in 2002, and is currently working towards the Ph.D. degree at the University of Auckland.

Since 2002, he has been an Assistant Engineer with Keam Holdem Associates, Auckland, New Zealand, which specializes in industrial microwave and RF heating.

Mr. Roelvink was the recipient of a Technology New Zealand Postgraduate Fellowship.

Allan G. Williamson (M'78–SM'83) received the B.E. and Ph.D. degrees in electrical engineering from the University of Auckland, Auckland, New Zealand, in 1970 and 1977, respectively.

Following a period with the New Zealand Broadcasting Corporation, he joined the Department of Electrical Engineering, University of Auckland, as a Lecturer in 1975, and became a Senior Lecturer in 1979, and an Associate Professor and Leader of the Radio Systems Group in 1985. In 1988, he became a Professor of telecommunications and is currently Department Head, having previously served as Department Head from 1989 to 1994, and Associate Dean (Research) with the Faculty of Engineering from 2000 to 2002. His early research was concerned with microwave passive devices, while more recently, he has been involved with mobile radio research, and is now involved with issues related to cellular radio, personal communications, and indoor wireless systems. In 1980, he was a Royal Society/Nuffield Foundation Scholar with the University of Birmingham, Edgsbaston, U.K. From 1984 to 1985, he was a Leverhulme Visiting Fellow with the University of Liverpool, Liverpool, U.K.

Prof. Williamson is a Fellow of the Institution of Electrical Engineers (IEE), U.K., and a Fellow of the Institution of Professional Engineers New Zealand. He has served as chairman of both the IEEE New Zealand North Section and the IEEE New Zealand Council.